Chemical Physics 422 (2013) 47–52

Contents lists available at SciVerse ScienceDirect

Chemical Physics

journal homepage: www.elsevier.com/locate/chemphys

Ultraviolet transient absorption, transient grating and photon echo studies of aqueous tryptophan

Ahmad Ajdarzadeh, Cristina Consani [1], Olivier Bräm, Andreas Tortschanoff [2], Andrea Cannizzo [3], Majed Chergui *

Ecole Polytechnique Fédérale de Lausanne (EPFL), Laboratoire de Spectroscopie Ultrarapide, ISIC, Station 6, FSB, CH-1015 Lausanne, Switzerland

ARTICLE INFO

Article history:
Available online 7 February 2013

Keywords:
Ultraviolet
Ultrafast
Transient absorption
Photon echo
Transient grating
Tryptophan

ABSTRACT

We compare UV transient grating (TG) experiments of aqueous tryptophan with transient absorption (TA) and fluorescence up-conversion measurements. The TG and TA signals show a bi-exponential rise with sub-ps and ps time constants, which are consistent with the fluorescence studies. Using experimental data, we provide an equation for the homodyne-detected TG signal, taking into account the sub-100 fs internal conversion of tryptophan after excitation. In addition, we measure a sub-100 fs homogeneous electronic dephasing time for tryptophan in water by the photon echo (PE) technique. These measurements provide a consistent picture of excited state dynamics of aqueous tryptophan that may serve as a basis for coherent 2D-UV spectroscopy of biosystems.

1. Introduction

Interrogating protein dynamics on the femtosecond to picosecond time scales has been extensively carried out with ultrafast optical spectroscopic techniques. Most studies [1–7] have consisted in impulsively exciting the bio-active centre of the protein (or artificially modified structures [8]), and monitoring its evolution in time using a time-delayed probe pulse. From its response, conclusions were drawn about the role of the protein environment. However, these studies do not probe the structure of the chromophore nor of its environment. For this X-ray studies are more useful as was demonstrated for the case of myoglobin by diffraction [9] or by X-ray absorption spectroscopy [10]. However, at present these techniques are limited in time resolution to the 50–100 ps pulse width of the synchrotron X-ray sources.

In recent years, multidimensional spectroscopy has emerged as a powerful tool that allows probing the dynamics of the native protein peptide chains by monitoring the IR absorption bands of specific chromophores (e.g. amide bands) that are part of it [11–15]. Pushing multidimensional spectroscopy into the visible range was pioneered by Fleming and co-workers [16–18] allowing to detect electronic couplings (e.g. excitonic effects) between chromophores within biological systems. In addition to probing electron or energy transfer among these chromophores, the analysis of the couplings can deliver information about the structure of the system as was recently demonstrated [19].

Probing the response of specific amino-acid residues upon excitation of the bio-active centre is another way to detect the protein response during a biological function. This necessitates probe pulses below 300 nm, which is the region where amino-acid residues absorb. Chergui and co-workers [20–22] used visible pump/UV probe transient absorption to monitor the response of tryptophan (Trp, which is the most abundant amino-acid residue in biological systems, has the highest absorption coefficient and is highly sensitive to the environment [23]) around photoexcited retinal in bacteriorhodopsin, while Mizutani et al. [24–26] used 220 nm probe pulses to monitor by resonance Raman spectroscopy the response of Trp in myoglobin after ligand photodissociation. Over the past few years, as complements to the above mentioned UV transient absorption tools, we have implemented ultrafast UV fluorescence up-conversion [27], which was used to study the relaxation dynamics of aqueous Trp [28], or tryptophan embedded in proteins, e.g. Cytochrome c [29,30].

Photon echo (PE) and transient grating (TG) experiments [31–36] hold the potential for increased sensitivity to environment effects, e.g., solvation dynamics, where the amplitude of the solvent-induced changes in absorption and/or the Stokes shift can be small. These techniques are also sensitive to both the ground and the excited state dynamics. While being widely used in the

* Corresponding author.
E-mail address: Majed.chergui@epfl.ch (M. Chergui).
[1] Now at Institut für Physikalische und Theoretische Chemie, Lehrstuhl für Physikalische Chemie I, Universität Würzburg Am Hubland, D-97074 Würzburg, Germany
[2] Now at CTR Carinthian Tech Research AG; Europastrasse 4/1, 9524 Villach/St. Magdalen, Austria.
[3] Now at the Institute of Applied Physics, University of Bern, Sidlerstr. 5, CH-3012, Bern, Switzerland.

0301-0104
http://dx.doi.org/10.1016/j.chemphys.2013.01.036

visible and IR spectral regions [31–35,37–42], PE and TG techniques have rarely been attempted in the UV due to, in particular, the significant non-resonant contributions from the solvent. Following the two-pulse PE experiments by Zimdars et al. [43], we implemented the three-pulse UV PE [44–46]. The implementation of these techniques is a necessary ingredient for the development of 2D coherent UV spectroscopies, which have been recently demonstrated on adenine [47]. A more detailed discussion about the ongoing developments in this area are found in Refs. [48] and [49]. 2D UV transient absorption spectroscopy has recently been implemented with very broad continua (>60 nm) [50] and used to investigate electron and energy transfer involving Trp in myoglobins [51]. Because of the importance of Trp in biological systems and in view of 2D coherent UV spectroscopy on them, the present paper compares the UV transient grating and photon echo experiments of aqueous tryptophan, with transient absorption and fluorescence up-conversion studies.

2. Experimental

The setup developed for the UV pump/broadband UV probe measurements was previously described [52]. Briefly, the output of a non-collinear optical parametric amplifier (NOPA) was doubled in a BBO crystal using the achromatic doubling scheme to obtain the broadband UV probe. The bandwidth of the generated UV light ranges between 20 nm and 60 nm, depending on the spectral window. Three measurements with different spectral windows were performed to cover the spectral range of interest (260–380 nm). The pump beam was generated by frequency doubling the output of a second NOPA in a 0.25 mm thick BBO crystal. The generated pump pulses have energies of around 100 nJ. The excitation wavelength was set at 287 nm and the measurements were performed under parallel polarisation. The temporal resolution of the set-up (cross-correlation of the pump and probe pulses) is about 160 fs.

The experimental set-ups for the Transient Grating (TG) and three-pulse photon echo peak shift (3PEPPS) measurements in the UV were presented in Refs. [44–46]. Briefly, after frequency doubling, we generate a central wavelength of 285–290 nm with a bandwidth of about 4 nm, at an average power of 1.6–2 mW at 30 kHz repetition rate (pulse energy of 50–66 nJ). A prism pair compression stage was used to compress the UV pulses before sending them to the photon echo set-up. UV pulses of 50–60 fs FWHM (Full Wave at Half Maximum) were used on the sample, yielding a temporal resolution of about 85 fs. In the photon echo set-up we divide the input beam into three beams of equal intensity, using thin beam splitters, with a time delay between them and focus them into a spot of about 100 μm. The photon echo signal is generated in the phase-matched direction ($k_s = -k_1 + k_2 + k_3$) where it is detected after blocking the incident beams. Detection of the generated signal is done in the two phase-matching directions simultaneously by means of two avalanche photodiodes.

Once the PE signal is detected, we do serial scans to get the PEPS (photon echo peak shift) results by scanning t_{12} for a sequence of t_{23} times. PEPS is defined as the value of t_{12} in which the maximum of the PE signal (for a given value of t_{23}) is detected. By detecting simultaneously the signals in the two directions $-k_1 + k_2 + k_3$ and $k_1 - k_2 + k_3$, we determined the photon echo peak shift as half the delay between the maxima (t_{12}^{max}) of the two curves. We can also perform the transient grating (TG) experiment which is the signal from a scan of t_{23} while $t_{12} = 0$.

The peak powers of the UV pulses on the sample for both photon echo and pump–probe set-ups are in the order of 10^8 W/cm^2, which is at least one order of magnitude weaker than the photoionization limit of Trp solution.

The solution of tryptophan was circulated with a mechanical pump to avoid sample degradation. The sample was a flow jet (for TG and PE experiments) and a flow cell (for TA experiments) with a thickness of 100 μm (or 200 μm). The concentration of Trp was chosen so as to have a sample absorbance of around 0.3 OD. For a sample thickness of 100 μm, this corresponds to a tryptophan concentration of around 8 mM in water.

3. Results

3.1. Transient absorption experiments

Fig. 1 shows a selection of transient spectra at different time delays. The transient absorption (TA) signal is positive over the entire observed spectral range, indicating the presence of a dominant contribution from excited state absorption (ESA). We observe a minimum of the signal between 265 and 290 nm. As shown in Fig. 1, this feature reflects the shape of the static absorption of the sample and is due to ground state bleaching (GSB). Similar measurements were already reported by Haacke and co-workers [53], with identical dynamics, who probed a wider spectral window ranging from 300 to 700 nm.

The time evolution of the signal at different wavelengths is shown in Fig. 2. It is described by a linear combination of exponential rise and decay components convoluted with the instrumental response function, and analysed with a global fit algorithm. The overall time evolution can be described in terms of four exponential contributions of characteristic times $\tau_1 = 250 \pm 20$ fs, $\tau_2 = 1.28 \pm 0.05$ ps, $\tau_3 = 31 \pm 6$ ps and $\tau_4 >> 100$ ps. In particular, we observe a bimodal rise of the signal with τ_1 and τ_2 for wavelengths between 280 nm and 350 nm and a decay with the same time constants at $\lambda < 280$ nm and $\lambda > 350$ nm. A Singular value decomposition (SVD) analysis confirms a very similar spectral evolution. In their study, Haacke and co-workers reported similar time scales for the τ_2–τ_3 components [53].

3.2. Transient grating and photon echo experiments

Since the TA signal is dominated by ESA, the higher states will most likely contribute to the Transient Grating (TG) signal. The TG experiments are performed with three identical pulses at 287 nm with a bandwidth of about 4 nm.

Fig. 3a and b shows, respectively, the long and short time evolution of the TG signal of tryptophan in water, normalised in

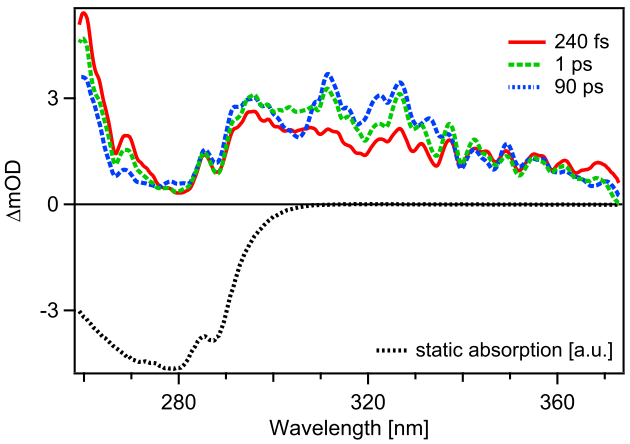

Fig. 1. Transient absorption of aqueous tryptophan excited at 287 nm at different delays after the excitation. The static absorption of the sample (dotted line, reversed sign) shows the expected shape of ground state bleaching in absence of excited state absorption.

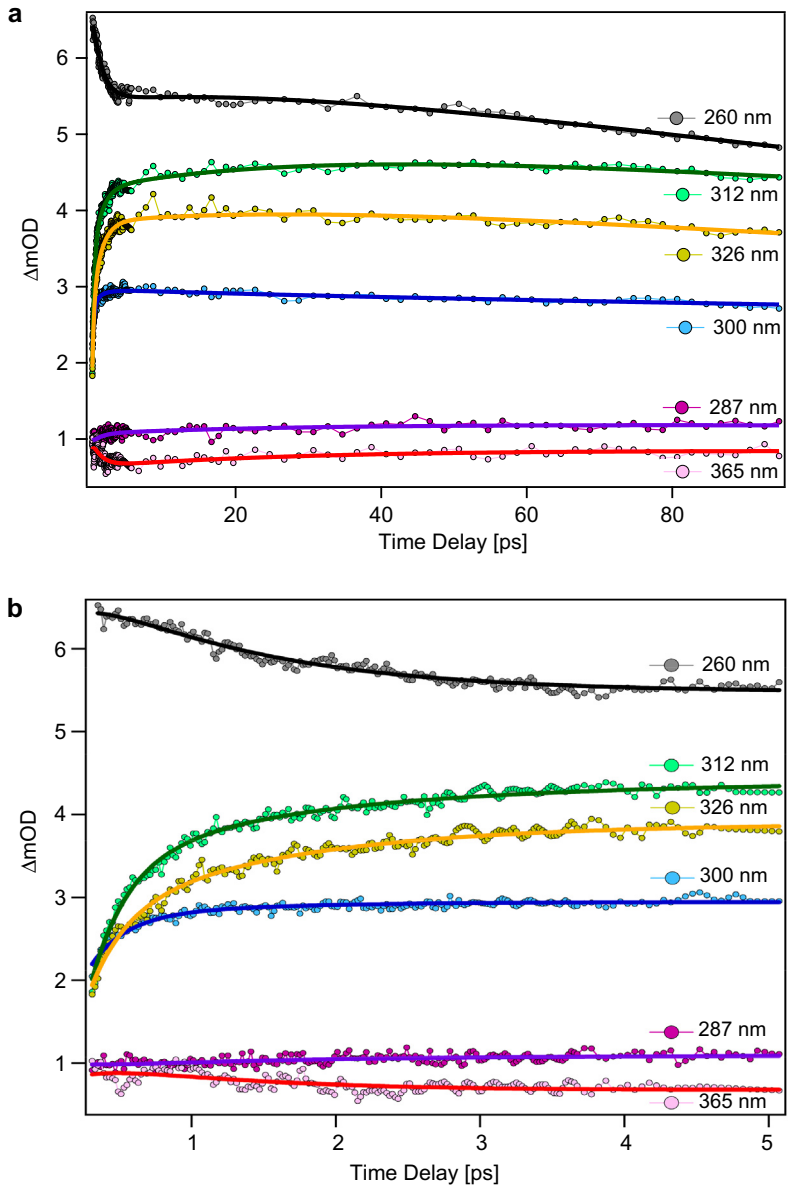

Fig. 2. Transient absorption kinetic traces of tryptophan in water at different probe wavelengths. (a) Long time scan; (b) short time scan. For purpose of clarity, the time trace at 260 nm was vertically shifted up by 1 mOD.

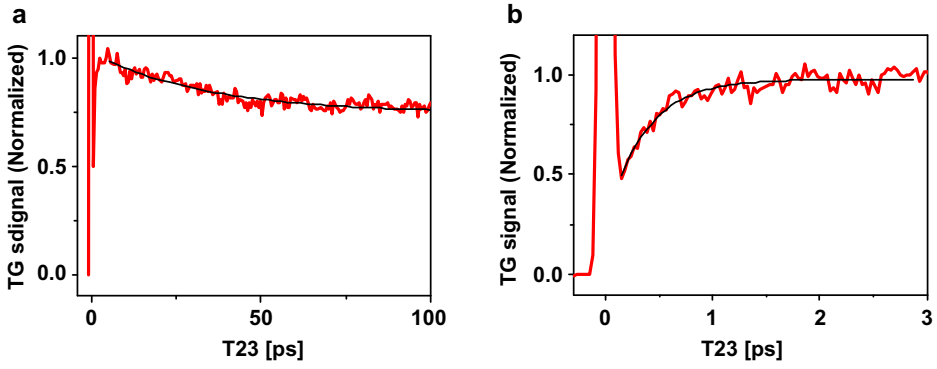

Fig. 3. Normalized TG signal of tryptophan in water in the phase-matched direction. (a) Long time signal. (b) Short time signal. All pulses were at 287 nm.

intensity. In a TG experiment, the first and second pulses overlap. The time delay between the second and third pulses is given by T_{23}. There is an intense peak at $T_{23} = 0$ which corresponds to the non-resonant contribution from water, appearing when the three

pulses temporally overlap each other [43–46]. At $T_{23} > 0$, this non-resonant signal vanishes and we detect the pure TG signal from tryptophan. The long-time scan (Fig. 3a) shows a decay that can be fitted by a single exponential of $\tau_{decay} = 32 \pm 3$ ps, while the short time scan shows a rise that is fitted by two components of $\tau_{rise\,1} = 200 \pm 50$ fs, $\tau_{rise\,2} = 1.0 \pm 0.2$ ps. These times are similar to the characteristic times found in the TA measurements. In addition, the fluorescence measurements on aqueous tryptophan [28], exhibited a Stokes shift of the emission spectrum with characteristic times of $\tau_1 = 160 \pm 40$ fs and $\tau_2 = 1.02 \pm 0.12$ ps, similar to those observed in TG and TA experiments. The Stokes shift of the emission was attributed to solvation dynamics of water. Table 1 compares the characteristic times of aqueous tryptophan dynamics measured by TG, TA and fluorescence up-conversion. As mentioned before, characteristic times observed by different techniques are close to each other. We will discuss this similarity in Section 4.

The slow decay (τ_3) corresponds to the rotational diffusion of the tryptophan molecules in water, in good agreement with the literature [28,54]. Since in a TG experiment we detect the intensity of generated third order signal (i.e., the amplitude squared of the third order non-linear optical response) without mixing it with an external field, the TG signal is called a homodyne detected signal. However, in a pump–probe (TA) experiment, we detect the superposition of the third order non-linear optical response with the probe pulse, we therefore monitor the amplitude of the third order signal and the TA signal is called a heterodyne detected signal [36]. Time-resolved fluorescence is also considered a heterodyne detected signal since in non-linear spectroscopy, it is represented as the superposition of the third order signal with vacuum fluctuations, which result in the spontaneous emission [36]. As a result, the TG signal is proportional to the square of the TA and the time-resolved fluorescence signal. We can obtain an equation for the TG signal, which is proportional to the square of the equation for time-resolved fluorescence signal, derived considering parallel polarizations for the excitation pulses and the detected fluorescence, and taking into account the rotational diffusion and neglecting the relaxation of the excited state population $\left(I_{Fluorescence} \propto \frac{5}{9} + \frac{4}{9} e^{-\frac{t}{\tau_{rot}}}\right)$ [55,56]:

$$I_{TG} \propto 0.309 + 0.197 e^{-\frac{t}{(\tau_{rot}/2)}} + 0.494 e^{-\frac{t}{\tau_{rot}}}, \quad (1)$$

In this equation τ_{rot} is the rotational decay time. Considering the above equation, one expects the TG signal to reach about 0.3 times its initial value, after complete rotational diffusion; however, the TG signal in Fig. 3(a) levels off at about 70% of its initial value. In order to explain this difference, we have to consider the photodynamics of tryptophan [23,57,58]. The lowest two excited singlet states (^1L_a and ^1L_b) are nearly degenerate and have perpendicular dipole moments [23,59]. Upon excitation with the first and second pulse in a TG experiment, both states are almost equally populated. The ratio of population at 290 nm excitation is $^1L_a/^1L_b$ = 55%/45% [28]. Internal conversion from ^1L_b to ^1L_a occurs in less than 100 fs [28,57,58], switching almost half of the dipole moments in the perpendicular direction, while the other half is still parallel to the direction of the excitation pulse polarisation. In this case, the value of the TG signal after rotational diffusion will no longer be described by Eq. (1). In order to estimate it, we use the fact that

Table 1
The characteristic times of aqueous tryptophan dynamics measured by TG, TA and fluorescence up-conversion (FlUC) techniques.

	TG	TA	FlUC
τ_1	200 ± 50 fs	250 ± 20 fs	160 ± 40 fs
τ_2	1.0 ± 0.2 ps	1.28 ± 0.05 ps	1.02 ± 0.12 ps
τ_3	32 ± 3 ps	31 ± 6 ps	34 ± 4 ps

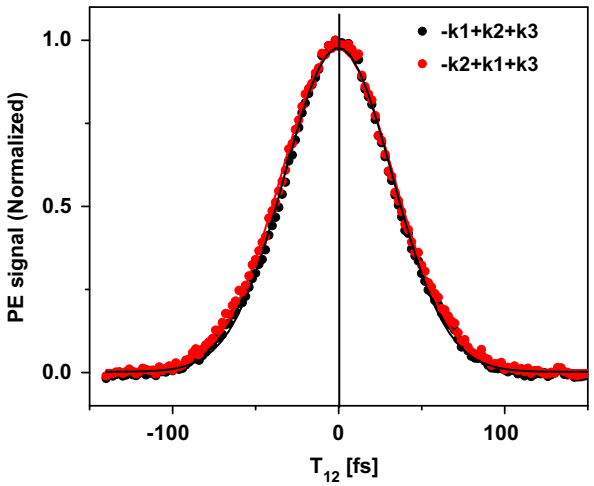

Fig. 4. PE signal of tryptophan in water at T_{23} = 100 fs, detected in two phase-matched directions (dotted lines). Signals are fitted with Gaussians (solid lines). Experiment is performed at 287 nm. T_{12} is the time delay between the first and second pulses and T_{23} is the time delay between the second and third pulses.

the fluorescence anisotropy of tryptophan in water just after internal conversion from ^1L_b to ^1L_a is about 0.1 [28,58]. Using the equation for fluorescence anisotropy [23]

$$r = \frac{I_{\parallel} - I_{\perp}}{I_{\parallel} + 2I_{\perp}}$$

where $I_{||}(I_{\perp})$ are the intensities of the fluorescence with the parallel (perpendicular) direction with respect to the polarisation of the excitation, one can calculate that the fluorescence intensity in the parallel direction just after internal conversion is about 1.33 times its intensity with polarisation in the perpendicular direction. After rotational diffusion, the fluorescence intensities with polarisation in the parallel and perpendicular directions become equal and amount to 1.11 times the initial fluorescence intensity in the perpendicular direction (the initial excess dipole moments in the parallel direction are distributed in 3 directions, then we have 0.33/3 = 0.11 times more dipole moments for each direction after rotational diffusion). As a result, the fluorescence intensity after rotational diffusion in the parallel direction should decay to 1.11/1.33 = 0.836 of its initial intensity. As mentioned above, the TG signal is a homodyne detected signal and is proportional to the square of the time-resolved fluorescence signal; therefore, we conclude that the normalised TG signal should decay to a value about $(0.836)^2$ = 0.7 after rotational diffusion, which is in good agreement with Fig. 3(a).

Fig. 4 shows the PE signal of tryptophan in water at T_{23} = 100 fs, detected in two phase-matched directions. It is seen that the signals are symmetric and can properly be fitted by a Gaussian line shape. This means (considering the temporal length of the UV pulses) a sub-100 fs homogeneous dephasing time for tryptophan in water at T_{23} = 100 fs [46]. This sub-100 fs dephasing time can result from the fact that excited tryptophan and water are polar molecules. Indeed, very fast dephasing times are common in polar solvation [35,60–64]. In addition, intramolecular dynamics such as internal conversion from ^1L_b to ^1L_a can also be the cause of the sub-100 fs dephasing time.[46]

4. Discussion

For a simple two-energy level system, one does not expect a rise of the TG signal, but a decay because all intramolecular and intermolecular relaxation phenomena should cause a dissipation of the spatial gratings in the ground and excited states. By fluorescence

UC measurements, it was found that about half of the total Stokes shift of tryptophan in water occurs instantaneously after excitation (Stokes shift of about 1700 cm^{-1} in a time shorter than 10 fs) [28]. This puts immediately the excited state population grating created by the first two pulses, out of the excitation window. In a simple two-level system, the third pulse would not interact with the excited state grating, consequently it would not contribute to the TG signal. However, in the presence of excited state absorption (ESA), which are resonant with the third pulse as found in the TA measurements, the latter pulse will also interact with the excited state grating, contributing to the TG signal. This results in the rise of the TG signal, giving the 200 fs and 1 ps components. It should be noted that any transition between the initial excited state and higher states will introduce a TG signal in the phase-matched direction, because the direction of the signal is given by that of the third pulse and the frequency-spatial grating created in the sample by interaction of the first two pulses.

As mentioned above, the TG signal is proportional to the square of the heterodyne-detected TA signal. As a result, the rotational diffusion should show up with two decay times of τ_{rot} and $\tau_{rot}/2$ and this applies to the rise times (τ_{rise} and $\tau_{rise}/2$). Therefore, we can provide a relation for the TG signal, including the rise and decay times and with a rough estimation of the coefficients:

$$I_{TG} \propto 0.75 + 0.23e^{-t/\tau_{rot}} - 0.24e^{-t/\tau_1} - 0.24e^{-t/\tau_2} + 0.018e^{-2t/\tau_{rot}} + 0.014e^{-2t/\tau_1} + 0.014e^{-2t/\tau_2} + 0.029e^{-t\left(\frac{\tau_1+\tau_2}{\tau_1\tau_2}\right)} \quad (2)$$

For deriving this equation, we used a TA signal as follows [55,56]:

$$I_{TA} \propto 0.87 + 0.14e^{-t/\tau_{rot}} - 0.12e^{-t/\tau_1} - 0.12e^{-t/\tau_2} \quad (3)$$

In Eq. (2), the pre-exponential coefficients are rough estimates from the fit of the TG and TA data. This introduces some errors but it does not change the temporal behaviour of the TG signal. We note that in Eq. (2) the last four terms are negligible. Therefore, it is clear that the rises and the decay on the TG signal will follow the same time characteristics (and not twice faster) as the TA and time-resolved fluorescence signals. It should be noted that the rise and decay dynamics are more pronounced in the TG signal compared to the TA signal, considering the coefficients in these two signals. This shows that the TG experiment is more sensitive to solvation and rotational dynamics than the TA experiment. The reason for this higher sensitivity is that we detect the intensity of signal by TG whereas in the TA experiment, we detect its amplitude.

As mentioned in the previous section, we observed a red shift of the emission spectrum with characteristic times of $\tau_1 = 160 \pm 40$ fs and $\tau_2 = 1.02 \pm 0.12$ps in the ultrafast fluorescence measurements of aqueous tryptophan, which we attributed to solvation dynamics [28]. Considering the above discussion and the similarity between the results of fluorescence UC and those of TG and TA measurements, we conclude that the origin of the rises observed in the TG and TA signals is solvation dynamics. A rise in the TA signal means an increase in ESA due to a better coupling of the initially excited state to the higher states by the probe pulse after completion of the Stokes shift. Therefore, solvation dynamics brings the initial excited state population at an energy or at an excited state configuration that offers a stronger coupling to higher states via either the third pulse in the TG experiment, or the probe pulse in the TA experiment.

5. Conclusions

In this paper, we presented the results of TG, TA and 3-pulse photon echo peak shift experiments on tryptophan in water and compared them with our previous fluorescence up-conversion measurements [28]. These four techniques give complementary and consistent information about the excited state dynamics. Solvation dynamics is observed as a Stokes shift in the fluorescence up-conversion, offering a favourable coupling between the initial excited state and higher states, which originates in the rises detected on the TG and TA signals. We provided an expression for the homodyne-detected TG signal taking into account the sub-100 fs internal conversion of tryptophan after excitation and considering experimental rise times and the rotational decay time. Because of excited state absorption, tryptophan cannot be considered a 2-level system in coherent spectroscopies, but this is compensated by an enhanced signal compared to transient absorption experiments. This is important for the development of coherent 2D UV spectroscopies.

Acknowledgements

This work was supported by grant 200020_121839 and the NCCR-MUST of the Swiss National Science Foundation (FNS).

References

[1] J. Helbing, L. Bonacina, R. Pietri, J. Bredenbeck, P. Hamm, F. van Mourik, F. Chaussard, A. Gonzalez-Gonzalez, M. Chergui, C. Ramos-Alvarez, C. Ruiz, J. Lopez-Garriga, Biophys. J. 87 (2004) 1881.
[2] X.J. Jordanides, M.J. Lang, X.Y. Song, G.R. Fleming, J. Phys. Chem. B 103 (1999) 7995.
[3] R. Jimenez, G. Salazar, K.K. Baldridge, F.E. Romesberg, Proc. Nat. Acad. Sci. USA 100 (2003) 92.
[4] J.L. Martin, M.H. Vos, Annu. Rev. Biophys. Biomol. Struct. 21 (1992) 199.
[5] P.M. Champion, F. Rosca, D. Ionascu, W.X. Cao, X. Ye, Faraday Discuss. 127 (2004) 123.
[6] F. Gruia, M. Kubo, X. Ye, D. Ionascu, C. Lu, R.K. Poole, S.R. Yeh, P.M. Champion, J. Am. Chem. Soc. 130 (2008) 5231.
[7] M. Kubo, F. Gruia, A. Benabbas, A. Barabanschikov, W.R. Montfort, E.M. Maes, P.M. Champion, J. Am. Chem. Soc. 130 (2008) 9800.
[8] B.E. Cohen, T.B. McAnaney, E.S. Park, Y.N. Jan, S.G. Boxer, L.Y. Jan, Science 296 (2002) 1700.
[9] F. Schotte, J. Soman, J.S. Olson, M. Wulff, P.A. Anfinrud, J. Struct. Biol. 147 (2004) 235.
[10] F.A. Lima, C.J. Milne, D.C.V. Amarasinghe, M.H. Rittmann-Frank, R.M. van der Veen, M. Reinhard, V.T. Pham, S. Karlsson, S.L. Johnson, D. Grolimund, C. Borca, T. Huthwelker, M. Janousch, F. van Mourik, R. Abela, M. Chergui, Review of Scientific Instruments 82 (2011) 063111.
[11] M.C. Asplund, M.T. Zanni, R.M. Hochstrasser, Proc. Nat. Acad. Sci. USA 97 (2000) 8219.
[12] Y.S. Kim, R.M. Hochstrasser, Proc. Nat. Acad. Sci. USA 102 (2005) 11185.
[13] J. Bredenbeck, J. Helbing, C. Kolano, P. Hamm, ChemPhysChem 8 (2007) 1747.
[14] P. Hamm, M.T. Zanni, Concepts and methods of 2d infrared spectroscopy, Cambridge University Pres, Cambridge; New York, 2011.
[15] A. Ghosh, R.M. Hochstrasser, Chem. Phys. 390 (2011) 1.
[16] T. Brixner, J. Stenger, H.M. Vaswani, M. Cho, R.E. Blankenship, G.R. Fleming, Nature 434 (2005) 625.
[17] Y.C. Cheng, G.S. Engel, G.R. Fleming, Chem. Phys. 341 (2007) 285.
[18] G.S. Schlau-Cohen, A. Ishizaki, G.R. Fleming, Chem. Phys. 386 (2011) 1.
[19] N.S. Ginsberg, J.A. Davis, M. Ballottari, Y.C. Cheng, R. Bassi, G.R. Fleming, Proc. Nat. Acad. Sci. USA 108 (2011) 3848.
[20] S. Schenkl, F. van Mourik, G. van der Zwan, S. Haacke, M. Chergui, Science 309 (2005) 917.
[21] S. Schenkl, F. van Mourik, N. Friedman, M. Sheves, R. Schlesinger, S. Haacke, M. Chergui, Proc. Nat. Acad. Sci. USA 103 (2006) 4101.
[22] J. Leonard, E. Portuondo-Campa, A. Cannizzo, F. van Mourik, G. van der Zwan, J. Tittor, S. Haacke, M. Chergui, Proc. Nat. Acad. Sci. USA 106 (2009) 7718.
[23] J.R. Lakowicz, Principles of fluorescence spectroscopy, 3rd ed., Springer, New York, 2006.
[24] M. Mizuno, N. Hamada, F. Tokunaga, Y. Mizutani, J. Phys. Chem. B 111 (2007) 6293.
[25] N. Fujii, M. Mizuno, Y. Mizutani, J. Phys. Chem. B 115 (2011) 13057.
[26] Y. Mizutani, M. Nagai, Chem. Phys. 396 (2012) 45.
[27] A. Cannizzo, O. Bräm, G. Zgrablic, A. Tortschanoff, A.A. Oskouei, F. van Mourik, M. Chergui, Opt. Lett. 32 (2007) 3555.
[28] O. Bräm, A.A. Oskouei, A. Tortschanoff, F. van Mourik, M. Madrid, J. Echave, A. Cannizzo, M. Chergui, J. Phys. Chem. A 114 (2010) 9034.
[29] O. Bram, C. Consani, A. Cannizzo, M. Chergui, J. Phys. Chem. B 115 (2011) 13723.
[30] C. Consani, O. Bram, F. van Mourik, A. Cannizzo, M. Chergui, Chem. Phys. 396 (2012) 108.

[31] M.H. Cho, N.F. Scherer, G.R. Fleming, S. Mukamel, J. Chem. Phys. 96 (1992) 5618.
[32] W.P. deBoeij, M.S. Pshenichnikov, D.A. Wiersma, J. Phys. Chem. 100 (1996) 11806.
[33] S.A. Passino, Y. Nagasawa, T. Joo, G.R. Fleming, J. Phys. Chem. A 101 (1997) 725.
[34] W.P. deBoeij, M.S. Pshenichnikov, D.A. Wiersma, Chem. Phys. Lett. 253 (1996) 53.
[35] T.H. Joo, Y.W. Jia, J.Y. Yu, M.J. Lang, G.R. Fleming, J. Chem. Phys. 104 (1996) 6089.
[36] S. Mukamel, Principles of nonlinear optical spectroscopy, Oxford University Press, New York, 1995.
[37] W.P. de Boeij, M.S. Pshenichnikov, D.A. Wiersma, Annu. Rev. Phys. Chem. 49 (1998) 99.
[38] J. Stenger, D. Madsen, P. Hamm, E.T.J. Nibbering, T. Elsaesser, J. Phys. Chem. A 106 (2002) 2341.
[39] M.H. Cho, J.Y. Yu, T.H. Joo, Y. Nagasawa, S.A. Passino, G.R. Fleming, J. Phys. Chem. 100 (1996) 11944.
[40] R. Agarwal, B.S. Prall, A.H. Rizvi, M. Yang, G.R. Fleming, J. Chem. Phys. 116 (2002) 6243.
[41] H. Bursing, D. Ouw, S. Kundu, P. Vohringer, Phys. Chem. Chem. Phys. 3 (2001) 2378.
[42] K. Ohta, K. Tominaga, Bull. Chem. Soc. Jpn. 78 (2005) 1581.
[43] D. Zimdars, R.S. Francis, C. Ferrante, M.D. Fayer, J. Chem. Phys. 106 (1997) 7498.
[44] A. Ajdarzadeh Oskouei, O. Bräm, A. Cannizzo, F. van Mourik, A. Tortschanoff, M. Chergui, J. Mol. Liq. 141 (2008) 118.
[45] A. Ajdarzadeh Oskouei, O. Bräm, A. Cannizzo, F. van Mourik, A. Tortschanoff, M. Chergui, Chem. Phys. 350 (2008) 104.
[46] A. Ajdarzadeh Oskouei, A. Tortschanoff, O. Bräm, F. Van Mourik, A. Cannizzo, M. Chergui, J. Chem. Phys. 133 (2010) 064506.
[47] C.H. Tseng, S. Matsika, T.C. Weinacht, Opt. Express 17 (2009) 18788.
[48] A. Cannizzo, Phys. Chem. Chem. Phys. 14 (2012) 11205.
[49] B.A. West, A.M. Moran, J. Phys. Chem. Lett. 3 (2012) 2575.
[50] G. Aubock, C. Consani, F. van Mourik, M. Chergui, Opt. Lett. 37 (2012) 2337.
[51] C. Consani, G. Auböck, F. van Mourik, M. Chergui, Science, http://dx.doi.org/10.1126/science.1230758.
[52] C. Consani, M. Premont-Schwarz, A. ElNahhas, C. Bressler, F. van Mourik, A. Cannizzo, M. Chergui, Angewandte Chemie-International Edition 48 (2009) 7184.
[53] D. Sharma, J. Leonard, S. Haacke, Chem. Phys. Lett. 489 (2010) 99.
[54] P. Mark, L. Nilsson, J. Phys. Chem. B 106 (2002) 9440.
[55] C. Cantor, P. Schimmel, Biophysical Chemistry, Part II: Techniques for the study of biological structure and function, W. H. Freeman and Company, 1980.
[56] A. Ajdarzadeh Oskouei, PhD Thesis - EPFL, Switzerland, (2011).
[57] D.P. Zhong, S.K. Pal, D.Q. Zhang, S.I. Chan, A.H. Zewail, Proc. Nat. Acad. Sci. USA 99 (2002) 13.
[58] X.H. Shen, J.R. Knutson, J. Phys. Chem. B 105 (2001) 6260.
[59] P.R. Callis, Fluorescence Spectroscopy 278 (1997) 113.
[60] M.L. Horng, J.A. Gardecki, A. Papazyan, M. Maroncelli, J. Phys. Chem. 99 (1995) 17311.
[61] J.S. Bresee, E.E. Mast, F.J. Coleman, M.J. Baron, L.B. Schonberger, M.J. Alter, M.M. Jonas, M.Y.W. Yu, P.M. Renzi, L.C. Schneider, JAMA J. Am. Med. Assoc. 276 (1996) 1563.
[62] B.M. Ladanyi, R.M. Stratt, J. Phys. Chem. 99 (1995) 2502.
[63] E.A. Carter, J.T. Hynes, J. Chem. Phys. 94 (1991) 5961.
[64] M.J. Lang, X.J. Jordanides, X. Song, G.R. Fleming, J. Chem. Phys. 110 (1999) 5884.